

## Evidence for Atomic Muon Capture by Fragments from Prompt Fission of Muonic $^{237}\text{Np}$ , $^{239}\text{Pu}$ , and $^{242}\text{Pu}$

W. U. Schröder, W. W. Wilcke, M. W. Johnson, D. Hilscher,<sup>(a)</sup> and J. R. Huizenga  
*Departments of Chemistry and Physics and Nuclear Structure Research Laboratory,  
 University of Rochester, Rochester, New York 14627*

and

J. C. Browne  
*Lawrence Livermore Laboratory, Livermore, California 94550*

and

D. G. Perry  
*Los Alamos Scientific Laboratory, Los Alamos, New Mexico 87544*

(Received 18 June 1979)

Muon capture in nuclei produced by prompt neutron emission and fission induced by radiationless transitions in the atomic cascade of muons bound to  $^{237}\text{Np}$ ,  $^{239}\text{Pu}$ , and  $^{242}\text{Pu}$  is reported. Lifetimes of muons bound to the targets, the  $(A-1)$  nuclei, and the neutron-rich fission fragments were measured. The lifetimes of the fission-fragment muonic atoms are consistent with the muon of the fissioning muonic atom going predominantly to the heavy-fragment atom.

There has been a long-standing puzzle of how to interpret the systematically higher disappearance rates of muons in actinide muonic atoms obtained from studies of the time distributions of muon-induced fission fragments as compared to measurements<sup>1</sup> involving muon-decay electrons and muon-capture neutrons and  $\gamma$  rays. Bloom<sup>2</sup> suggested an excitation of shape-isomeric nuclear states during the muonic cascade, introducing an additional fission channel to be responsible for the apparent discrepancies in the data. In contrast, Hadermann<sup>3</sup> emphasized the importance of sequential atomic muon capture by fragments resulting from prompt muon-induced fission. As is experimentally well established, high-energy muonic  $E1$  or  $E2$  cascade transitions to the  $1s$  ground state may proceed by radiationless excitation of the nucleus leading to prompt fission or neutron emission in the presence of the muon. The muon then remains on the daughter isotope or, in a fission event, on one of the fragments, if not ejected during the fission or subsequent de-excitation processes. From the muonic  $1s$  level of such a fragment, the muon then disappears with a characteristic rate lower than that of an actinide, an effect enhanced by the large  $A/Z$  ratio of fission fragments.

Evidence in support of Hadermann's proposal has been obtained by Ganzorig *et al.*<sup>4</sup> by measuring muon-decay electrons in coincidence with prompt-fission fragments and by Wilcke *et al.*<sup>1</sup> by observing long-lived components in the time

spectra of neutrons emitted from the highly fissile muonic  $^{237}\text{Np}$ ,  $^{239}\text{Pu}$ , and  $^{242}\text{Pu}$ . The present experiments, employing the latter targets and a more sensitive fission-fragment-neutron coincidence technique, were undertaken in order to demonstrate that the evidence for the recently discovered mechanism is independent of both the experimental technique and nuclide. Such studies have also the interesting potential of extending the systematics of muon capture into regions of short-lived nuclei and may provide information on the coupling between muonic and collective degrees of freedom.

The experiments were performed with the stopped-muon channel of the Clinton P. Anderson Meson Physics Facility (LAMPF). As indicated in Fig. 1 showing a schematic of the apparatus, muons entered a counter telescope (1234) and stopped in a fission chamber containing Ti foils on which  $^{237}\text{Np}$ ,  $^{239}\text{Pu}$ , and  $^{242}\text{Pu}$  targets were deposited as oxides. Six NE-213 neutron detectors,<sup>5</sup> surrounding the fission chamber at a mean distance of 10 cm, were used to detect neutrons in coincidence with fission fragments.

Typical results of an experimental run for  $^{239}\text{Pu}$  are displayed in Fig. 2, showing the fission-fragment-neutron coincidence rate plotted in a two-dimensional diagram versus the times  $t_{\text{fission}}$  and  $t_{\text{neutron}}$  between a  $\mu$  stop in the target located in the fission chamber and the detection of the resulting coincident fission fragment and neutron, respectively. Three ridges are clearly observa-

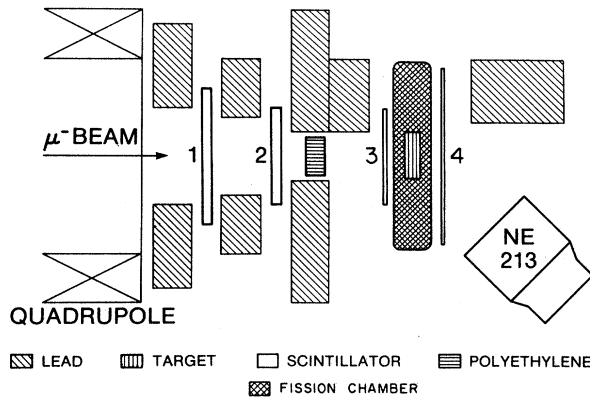


FIG. 1. Schematic diagram of experimental setup. For explanation, see text.

ble, extending from the dominant prompt peak towards longer times. Ridge A is due to delayed muon-capture-induced fission of  $^{239}\text{Pu}$ , where a fission fragment is detected in prompt coincidence with a neutron associated with de-excitation of either of the two fragments. Ridge B results from prompt emission of a neutron in a radiationless process followed by muon-capture-induced fission of the daughter isotope  $^{238}\text{Pu}$ . Ridge C is due to prompt muon-induced fission of the target followed by muon capture in one of the fission fragments as identified by the appearance of a delayed neutron. This latter ridge is of primary interest to the present study.

Projecting ridges A and B onto the axis given by  $t_{\text{fission}}$  and ridge C onto that corresponding to  $t_{\text{neutron}}$ , one obtains the time distributions of the three classes of events such as shown in Fig. 3 for a sample run on  $^{239}\text{Pu}$ , where a constant background has been subtracted. The distributions reflect the lifetimes of muonic  $^{239}\text{Pu}$  (A), of muonic  $^{238}\text{Pu}$  (B), and of the muonic fission fragments (C). The experimental lifetimes of the different types of events as obtained from exponential fits to the data of several runs are displayed in Table I. The data in ridge (B) illustrate for the first time a new technique for the measurement of the lifetime of actinide muonic atoms with one neutron removed from the target (although statistics are presently inadequate for a precise lifetime determination).

Whereas experimental slopes of the time distributions are very similar for the target and its daughter produced by prompt neutron emission, the distributions corresponding to the fission fragments (C) indicates a much lower rate of disap-

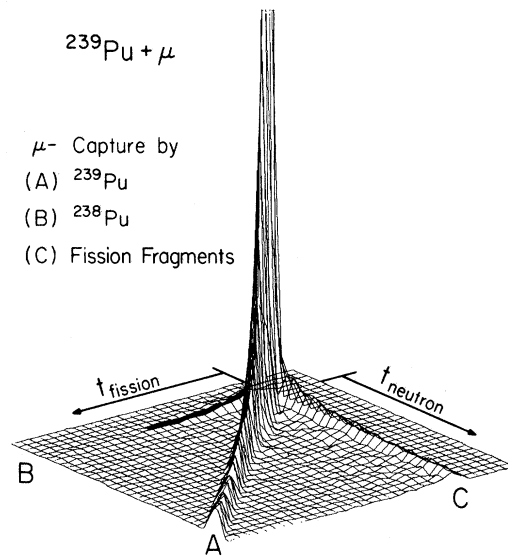


FIG. 2. Fission-fragment-neutron coincidence rate plotted in a two-dimensional diagram vs the times  $t_{\text{fission}}$  and  $t_{\text{neutron}}$  between the arrival of a muon in the fission chamber and the detection of the fission fragment and neutron, respectively (see text).

pearance of the muon. The latter distributions were analyzed with a theoretical fit function including a random-time background and two exponentials corresponding to muon capture in the

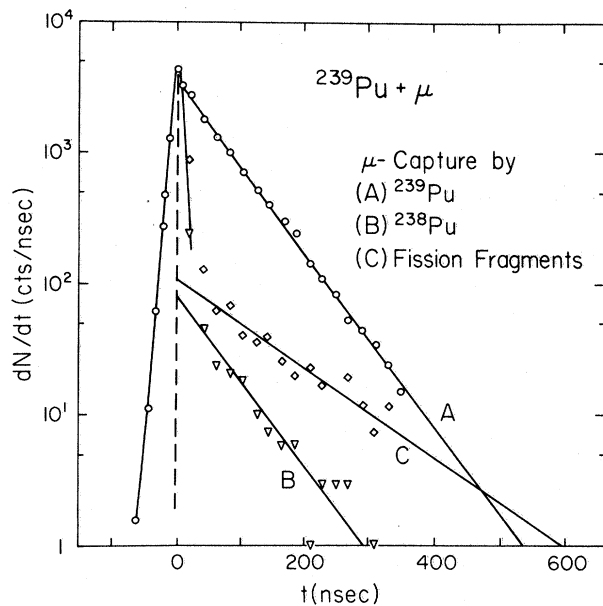


FIG. 3. Decay curves of the three classes of events obtained by projecting the different ridges of Fig. 2 onto the respective time axes (see text).

TABLE I. Mean lifetimes in nanoseconds of muons in the target muonic atoms,  $\tau(A)$ ; in the muonic daughter atom after emission of a neutron,  $\tau(A-1)$ ; and in muonic fission fragments,  $\tau(\text{f.f.})$ .

Target	$\tau(A)$	$\tau(A-1)$	$\tau(\text{f.f.})$
$^{237}\text{Np}$	$71.3 \pm 0.9$	$71 \pm 10$	$126 \pm 7$
$^{239}\text{Pu}$	$70.1 \pm 0.7$	$70 \pm 10$	$133 \pm 7$
$^{242}\text{Pu}$	$75.4 \pm 0.9$	$75 \pm 10$	$133 \pm 9$

light and the heavy fission fragments. From the data, however, only one exponential component

$$\lambda_{\text{CP}} = KZ_{\text{eff}}^4 \left(1 - \frac{\epsilon_{\mu}}{m_{\mu}}\right) \left(1 - \frac{m_{\mu} - \epsilon_{\mu}}{m_N}\right) \left[1 - 0.03 \frac{A}{2Z} + 0.25 \frac{A-2Z}{2Z} - 3.24 \left(\frac{A-Z}{2A} + \frac{|A-2Z|}{8ZA}\right)\right], \quad (1)$$

where the notation is that of Ref. 1. The theoretical mean muonic lifetime  $\tau$  is given by  $\tau = (\lambda_{\text{CP}} + \lambda_0)^{-1}$ , where  $\lambda_0 \approx 4.55 \times 10^5 \text{ sec}^{-1}$  is the muon-decay rate. Application of Eq. (1) to representative nuclei produced in low-energy fission (after  $n$  emission) reveals that heavy fragments have characteristic lifetimes  $\tau_H \approx 120 \text{ nsec}$ , while the corresponding lifetimes for typical light fragments are  $\tau_L \approx 200 \text{ nsec}$ . The experimental muonic lifetimes  $\tau(\text{f.f.})$  for fission fragments displayed in Table I agree well with the estimated value of  $\tau_H$  indicating that, after a prompt-fission process, the muon is dominantly captured by the heavy fragment. This result for the prompt fission of  $^{237}\text{Np}$ ,  $^{239}\text{Pu}$ , and  $^{242}\text{Pu}$  is in agreement with measurements of Ganzorig *et al.*<sup>4</sup> for  $^{232}\text{Th}$  and  $^{238}\text{U}$  obtained with a different technique. An additional piece of information supporting this interpretation is seen in the fact that the muonic lifetimes for fission fragments are equal within the errors for targets ranging from  $^{232}\text{Th}$  to  $^{242}\text{Pu}$ , whereas significant variations should have been observable in the case of dominant muon capture by the light fragment. Average masses of the light fission products are observed<sup>7</sup> to vary approximately linearly with the mass of the fissioning nucleus, whereas those of the heavy fragments are almost constant for the actinide region.

The absence of sequential muon capture by the light fission fragments suggested by these experiments bears some implications on the dynamics of the coupled system comprised of the muon and fissioning nucleus. This subject is presently being studied by various theoretical groups. If the nuclear fission mode is highly damped, the nuclear collective velocity from saddle to scission is expected to be much smaller than typical ve-

was found with statistical significance, restricting a possible contribution from a second component to less than 10%. The muonic fission fragment lifetimes are also collected in Table I.

Given the above results, it is appropriate to determine the identity of the "average fission fragment" which captures the muon, by a comparison with predicted lifetimes of muons bound to typical fission fragments. Such predictions may be made with the Goulard-Primakoff formula<sup>6</sup> which describes on the average the muon-capture rates for a wide range of elements. This formula is given by

locities of the muon in its ground state ( $v_{\mu} \approx 0.36c$ ). Such a situation, where the rearrangement of the muonic orbit occurs adiabatically with respect to the fission process, would result in a predominant capture of the muon into the 1s state of the heavy fragment. However, calculations of electron inner-shell ionization of fission products during nuclear fission<sup>8</sup> and an experiment providing some evidence for muon ejection<sup>9</sup> during radiationless-transition fission, indicate that the above view based on consideration of velocities alone may be oversimplified.<sup>10</sup> Information about this subject, as well as the time scale associated with the fission process, may be obtained by a search for muonic x rays (Doppler shifted) from muonic fission fragments.

In summary, evidence is presented in this work for the dominance of sequential muon capture by the heavy fragments produced in prompt muon-induced fission of muonic actinides. The resulting probabilities and muonic lifetimes associated with this process are consistent with the observations of long-lived components in the time distributions of neutrons from these muonic atoms. Excitation of isometric states during the muon cascade have not been observed in the present experiment. It is obvious from the data such as illustrated in Fig. 2, that true muon-capture rates of actinides are only obtained from experiments eliminating contributions from muon capture in products of prompt radiationless processes. The present experiments are clearly consistent with the predictions of the Goulard-Primakoff theory for muon-capture rates for nuclei far off the  $\beta$ -stability valley. However, a more definitive test of the model would require a coinci-

dence experiment, in which the prompt-fission fragments are identified with respect to their  $A$  and  $Z$ .

This work was supported by the U. S. Department of Energy. The authors wish to thank L. E. Agnew, B. R. Rector, and the LAMPF technical staff for their hospitality and assistance.

<sup>(a)</sup>On leave of absence from the Hahn-Meitner Institut, Berlin, West Germany.

<sup>1</sup>W. W. Wilcke, M. W. Johnson, W. U. Schröder, J. R. Huizenga, and D. G. Perry, Phys. Rev. C **18**, 1452 (1978), and references cited therein.

<sup>2</sup>S. D. Bloom, Phys. Lett. **48B**, 470 (1974).

<sup>3</sup>J. Hadermann, Phys. Lett. **67B**, 35 (1977).

<sup>4</sup>Dz. Ganzorig, P. G. Hansen, T. Johansson, B. Jonsson, J. Konijn, T. Krogulski, V. D. Kuznetsov, S. M. Polikanov, G. Tibell, and L. Westgaard, Phys. Lett. **77B**, 257 (1978).

<sup>5</sup>Highly efficient  $\gamma$ - $n$  pulse-shape discrimination circuits were provided and manufactured by the Hahn-Meitner Institut, Berlin, West Germany.

<sup>6</sup>D. Goulard and H. Primakoff, Phys. Rev. C **10**, 2034 (1974).

<sup>7</sup>R. Vandenbosch and J. R. Huizenga, *Nuclear Fission* (Academic, New York and London, 1973).

<sup>8</sup>J. V. Noble, Nucl. Phys. **A187**, 568 (1972).

<sup>9</sup>G. E. Belovitskii, Yu. A. Batusov, and L. V. Sukhov, Pis'ma Zh. Eksp. Teor. Fiz. **27**, 662 (1978) [JETP Lett. **27**, 625 (1978)].

<sup>10</sup>Yu. N. Demkov, D. F. Zarestskii, F. F. Karpeshin, M. A. Listengarten, and V. N. Ostrovskii, Pis'ma Zh. Eksp. Teor. Fiz. **28**, 287 (1978) [JETP Lett. **28**, 263 (1978)].

## Study of the Reactions $^{46,48}\text{Ti}(^{14}\text{C},^{16}\text{O})^{44,46}\text{Ca}$ and $^{50,52}\text{Cr}(^{14}\text{C},^{16}\text{O})^{48,50}\text{Ti}$ at 51 MeV

J. C. Peng, Nelson Stein, J. W. Sunier, D. M. Drake,

J. D. Moses, J. A. Cizewski, and J. R. Tesmer

*University of California, Los Alamos Scientific Laboratory, Los Alamos, New Mexico 87545*

(Received 11 June 1979)

The first measurements are reported for  $(^{14}\text{C},^{16}\text{O})$  two-proton pickup reactions. Angular distributions for transitions up to  $\sim 3.5$  MeV excitation in  $^{44,46}\text{Ca}$  and  $^{48,50}\text{Ti}$  were obtained with a 51-MeV  $^{14}\text{C}$  beam. The angular distributions exhibit a characteristic  $l$  dependence. Significant two-proton-hole configurations are found in the first excited  $0^+$  states of  $^{44}\text{Ca}$  (1.88 MeV) and  $^{46}\text{Ca}$  (2.42 MeV). Evidence is presented for multistep excitation of the first  $2^+$  states, especially in  $^{44}\text{Ca}$  and  $^{46}\text{Ca}$  where one-step transitions are expected to be inhibited.

Two-nucleon transfer reactions provide a basic experimental method for studying pairing correlations in nuclei.<sup>1,2</sup> A large amount of data already exists for the stripping and pickup of two neutrons by use of  $(t, p)$  and  $(p, t)$  reactions, and some very limited data are also available on two-proton stripping by the  $(^3\text{He}, n)$  reactions. However, there are almost no data of spectroscopic usefulness for two-proton pickup, because of the experimental difficulties of the  $(n, ^3\text{He})$  reaction, which is the obvious light-ion reaction to perform. The  $(^{18}\text{O}, ^{20}\text{Ne})$  reaction<sup>3,4</sup> has been investigated as a possible alternative to the  $(n, ^3\text{He})$  reaction, but unfortunately, the strong excitation of low-lying states of  $^{20}\text{Ne}$  often prevents clean separation of excited states of the final nuclei under study. In addition, strong coupling between the ground and low-lying collective states in both  $^{18}\text{O}$  and  $^{20}\text{Ne}$  increases the likelihood of complicated multistep processes in the  $(^{18}\text{O}, ^{20}\text{Ne})$  reactions,

thereby making the extraction of spectroscopic information difficult.

Since the first excited states in both  $^{14}\text{C}$  and  $^{16}\text{O}$  occur above 6 MeV excitation, the principal difficulties encountered with  $(^{18}\text{O}, ^{20}\text{Ne})$  are not expected in the  $(^{14}\text{C}, ^{16}\text{O})$  reaction, or at least they should be greatly reduced. In addition, this reaction possesses high positive  $Q$  values that are kinematically very favorable. For these reasons, it is of interest to explore experimentally the properties of the  $(^{14}\text{C}, ^{16}\text{O})$  reaction and to determine its usefulness as a source of proton-pairing information.

To perform the experiment,  $^{14}\text{C}$  ions were produced<sup>5</sup> in a sputter source and then accelerated to an energy of 51 MeV in a Van de Graaff accelerator. Self-supporting targets of  $^{46,48}\text{Ti}$  and  $^{50,52}\text{Cr}$  of approximately  $100\text{-}\mu\text{g}/\text{cm}^2$  thickness were bombarded with a beam intensity of 200 nA. The  $^{16}\text{O}$  reaction products were detected and iden-